Journal of Biomechanics 90 (2019) 58–64

Contents lists available at ScienceDirect

Journal of Biomechanics

journal homepage: www.elsevier.com/locate/jbiomech
www.JBiomech.com

An actuated dissipative spring-mass walking model: Predicting human-like ground reaction forces and the effects of model parameters

Tong Li [a], Qingguo Li [b], Tao Liu [a,*]

[a] State Key Laboratory of Fluid Power and Mechatronic Systems, School of Mechanical Engineering, Zhejiang University, 310027 Hangzhou, China
[b] Department of Mechanical and Materials Engineering, Queen's University, Kingston, ON, Canada

ARTICLE INFO

Article history:
Accepted 17 April 2019

Keywords:
Human walking
Spring-mass model
Actuated
GRF
Optimization

ABSTRACT

Simple models are widely used to understand the mechanics of human walking. The optimization-based minimal biped model and spring-loaded-inverted-pendulum (SLIP) model are two popular models that can achieve human-like walking patterns. However, ground reaction forces (GRF) from these two models still deviate from experimental data. In this paper, we proposed an actuated dissipative spring-mass model by integrating these two models to realize more human-like GRF patterns. We first explored the function of stiffness, damping, and weights of both energy cost and force cost in the objective function and found that these parameters have distinctly different influences on the optimized gait and GRF profiles. The stiffness and objective weight affect the number and size of peaks in the vertical GRF and stance time. The damping changes the relative size of the peaks but has little influence on stance time. Based on these observations, these parameters were manually tuned at three different speeds to approach experimentally measured vertical GRF and the highest correlation coefficient can reach 0.983. These results indicate that the stiffness, damping, and proper objective functions are all important factors in achieving human-like motion for this simple walking model. These findings can facilitate the understanding of human walking dynamics and may be applied in future biped models.

1. Introduction

Walking is one of the most common locomotion patterns for daily living. Healthy humans walk in a similar pattern with typical features: an alternating double support (DS) phase and single support (SS) phase, a double-peak ground reaction force (GRF) profile, etc. (Whittle, 2007; Winter, 2009). Modeling and simulation, especially predictive simulations, have been widely used to understand the underlying mechanism of human walking and predict human interaction with external environments (Hicks et al., 2015). An ultimate goal of walking models is to replicate human walking as close as possible, in order to apply these models to studies related to humanoids, exoskeletons and so on. Numerous models have been proposed in literature and they differ from each other in structure and complexity. Since the human body is extremely complex, different levels of simplification result in models with varying complexity. According to the complexity level, these models can be roughly divided into three categories: center-of-mass level models, giving information about center-of-mass trajectory and external GRF force; joint-level models (Ren et al., 2005; Xiang et al., 2012), providing additional information on joint kinematics and kinetics; and muscular-skeletal models (Anderson and Pandy, 2001; Song and Geyer, 2015), giving further information including muscle actuation and coordination. Complicated models have the potential to produce similar walking patterns as humans and can provide more information on human movements. However, they suffer from difficulties that arise from control methods: especially when using optimization techniques due to the "curse of dimensionality" (Bellman, 2003). On the other hand, center-mass level models remain simple and are able to offer many important insights about human walking (Alexander, 1995; Kuo, 2001).

At the center-mass level, the classic inverted pendulum model (Cavagna et al., 1976; McGrath et al., 2015) can only represent the SS phase and thus cannot generate a full walking step containing a DS phase. Collision-based models include the passive dynamic walker (Mcgeer, 1990), the simplest walking model (Garcia et al., 1998; Kuo, 2002) and some other anthropomorphic biped models (Alexander, 1995; Kuo, 2001). These models are limited to an instantaneous DS phase and therefore result in an infinitely large GRF force. There are two representative models that

* Corresponding author at: Zhejiang University, 38 Zheda Road, 310027 Hangzhou, China.
E-mail addresses: zjulitong@zju.edu.cn (T. Li), ql3@queensu.ca (Q. Li), liutao@zju.edu.cn (T. Liu).

https://doi.org/10.1016/j.jbiomech.2019.04.028
0021-9290/

can achieve human-like walking patterns with the double-peak GRF pattern: the spring-loaded-inverted-pendulum (SLIP) model (Geyer et al., 2006) and the minimal biped model (Srinivasan and Ruina, 2006). They are both extremely simple, only containing a point mass and two massless legs, but differ from each other significantly. The SLIP model is totally passive and includes two springy massless legs. Periodical walking can be obtained by forward integration from a proper initial condition, requiring no actuation and energy input since the spring is energy conservative. Tuning parameters such as spring constants and the angle of attack can also achieve various different walking patterns (Rummel et al., 2010). In contrast, the minimal biped model is active and includes a translational actuator in each leg. Actuation forces are obtained from the optimization of energy cost on mechanical work. The resultant walking patterns of this model are similar to the impulsive walking model with a larger GRF in DS phase. Adding a cost from actuation force derivatives (Rebula and Kuo, 2015), or a bound on the force derivatives (Srinivasan, 2010), the model achieved smoother walking gait patterns similar to human walking.

It's indeed already impressive that the SLIP model and minimal biped model can achieve human-like walking patterns with such simple structures. However, the minimal biped model tends to predict higher force at the mid-stance and it could be a small peak rather than a trough (Rebula and Kuo, 2015). On the contrary, the SLIP model usually gives deeper trough value (Geyer et al., 2006; Rummel et al., 2010). This inspires combining components of the SLIP model and the minimal biped model to achieve closer predictions of human walking patterns in term of GRF pattern. This idea was tested by putting a spring in series with the leg actuators, which was claimed able to realize the human-like GRF pattern (Srinivasan, 2010). However, the comparison was only made qualitatively in that paper. In addition, a flaw of this combined model is that leg actuator power resulted in a value near zero, which indicates that it still acted as the SLIP model. This is perhaps due to the fact that the spring mechanism is energy conservative and therefore the optimizer minimizes the actuation power to zero.

In this paper, we integrate the SLIP model and the minimal biped model, proposing an actuated dissipative spring-mass model to achieve more human-like walking patterns. Beyond the spring-actuator legs in (Srinivasan, 2010), a damping element is added in parallel with the spring mechanism which allows energy dissipation and requires power input from actuation. We quantitatively compared the model-predicted GRF with empirical walking data, at three speeds, to examine the function of each element and evaluate the performance of the model. We expect that the spring-damping unit can help to achieve a more human-like walking pattern and the proposed model may be applied in further studies on the understanding human walking mechanics and the design of assistive devices.

2. Methods

2.1. Model description

Our model is based on the minimal biped model (Srinivasan and Ruina, 2006) with spring-damping units added to each leg, as shown in Fig. 1. The human body is considered as a point mass and is supported by two massless legs. A telescoping actuator is embedded in series with the spring-damping unit in each leg and provides axial forces only. We assume human walking as periodical and symmetric between steps and thus we only consider one step in the model. Without loss of generality, we name the two legs as Leg1 and Leg2 (Fig. 1). The position of the body center of mass (CoM) is denoted as (x_c, y_c). The orientation of the two legs is described as

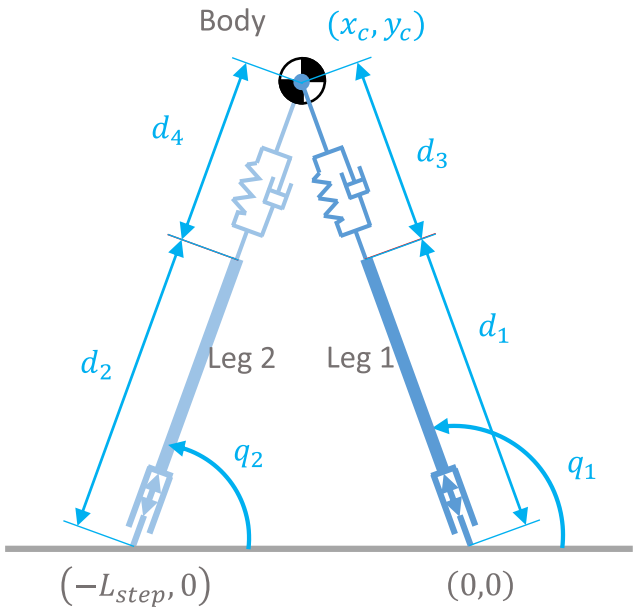

Fig. 1. The actuated dissipative spring-mass model which consists of a point mass and two massless legs. Each leg has a spring-damping unit in series with a translational actuator. A step is considered with the leading leg touching down at the position of (0,0). The trailing leg starts from the position of $(-L_{step}, 0)$, where L_{step} is the step length.

$q_1 = \pi/2 - \text{atan}(x_c/y_c)$ and $q_2 = \pi/2 - \text{atan}((x_c + L_{step})/y_c)$, where L_{step} is the step length. Each leg contains two parts, namely the actuator part (length of d_1 and d_2) and spring-damping unit part (length of d_3 and d_4). During the DS phase, the system can be described by the generalized coordinates of $x_{DS} = [x_c, y_c, d_3, d_4]^T$. From the linear momentum balance of the body mass, we have:

$$\begin{bmatrix} M & 0 \\ 0 & M \end{bmatrix} \begin{bmatrix} \ddot{x}_c \\ \ddot{y}_c \end{bmatrix} = \begin{bmatrix} \cos q_1 & \cos q_2 \\ \sin q_1 & \sin q_2 \end{bmatrix} \begin{bmatrix} F_1 \\ F_2 \end{bmatrix} - \begin{bmatrix} 0 \\ M \end{bmatrix} g \tag{1}$$

where M is the mass of the body, $F_1 = -\left(kd_3 - cd_3\dot{d}_3\right)$ and $F_2 = -\left(kd_4 - cd_4\dot{d}_4\right)$ are the forces in Leg1 and Leg2 respectively, and$k$ and c are the stiffness and damping value of the legs, respectively. The spring-damper unit is at resting length ($d_3 or d_4 = 0$) at heel-strike and toe-off. In our model, the spring-damping force is calculated with the Hunt-Crossley contact force model (Hunt and Crossley, 1975), rather than the Kelvin-Voigt model (for example $F_1 = -(kd_3 + c\dot{d}_3)$). This is because the Kelvin-Voigt model suffers from the problem of discontinuous force at the beginning and the end of contact due to damping (Flores and Lankarani, 2016; Pappalardo et al., 2016), while the Hun-Crossley model ensures zero contact force at the resting length.

We have four DOFs in DS phase but only have two equations of motion (EOM) as in (1). The second derivatives of spring length $\ddot{d}_3$ and $\ddot{d}_4$ are controlled by the leg actuators and theoretically can be any values as the legs are massless. Thus, we also include $\ddot{d}_3$ and $\ddot{d}_4$ as our design variables in the optimization process and in this way we can obtain the system states ($\left[x_c, \dot{x}_c, y_c, \dot{y}_c, d_3, \dot{d}_3, d_4, \dot{d}_4\right]^T$) by integrating $\left[\ddot{x}_c, \ddot{y}_c, \ddot{d}_3, \ddot{d}_4\right]^T$. During the SS phase, the generalized coordinates are $x_{SS} = [x_c, y_c, d_3]^T$. We still have two EOMs same as (1) only with $F_2 = 0$. Thus we include $\ddot{d}_3$ as the design variables in order to simulate the system forward.

2.2. Optimization implementation

Given a certain combination of model parameters (M, k, c, and maximal leg length L_{max}) and specified gait parameters (velocity v and L_{step}), there would be innumerable methods of controling the model to achieve a periodical gait. Thus an optimal control problem is formulated to search for an "optimal" gait. The optimization objective consists of two parts: the energy cost (J_w) computed from mechanical work performed by leg actuators and the generalized force cost (J_f) which is expected to penalize high rates of force generation (Rebula and Kuo, 2015). A weight α is used to adjust the influence of each cost in the total objective. Therefore the objective function (J) to be minimized is defined as:

$$J = (1-\alpha)J_w + \alpha J_f \tag{2}$$

$$J_w = \int_0^{T_{step}} \left(\left| F_1 \cdot \dot{d}_1 \right| / b_1 + \left| F_2 \cdot \dot{d}_2 \right| / b_2 \right) dt \tag{3}$$

$$J_f = \sqrt{\int_0^{T_{step}} \left(\left| \ddot{F}_1 \right|^2 + \left| \ddot{F}_2 \right|^2 \right) dt} \tag{4}$$

where T_{step} is the time of a step. Humans perform positive and negative mechanical work at different efficiency (Margaria, 1976) and b_i equals to 0.25 if $F_i \cdot \dot{d}_i > 0$ and 1.20 if $F_i \cdot \dot{d}_i < 0$, $i = 1, 2$. Further implementation details can be found in Supplemental Materials.

2.3. Comparison between model predictions and experimental data

Nine subjects (weight = 69.7±8.23 kg, height = 1.74±0.06 m) were recruited to walk freely on an instrumented treadmill (Bertec, USA) at three speeds (1, 1.25, 1.5 m/s). The experiment was approved by the Committee of Ethics of Zhejiang University and all subjects signed informed consent prior to the testing. GRFs were recorded at 1000 Hz and filtered with a 4th order Butterworth filter with a cut-off frequency of 20 Hz. The gait events are recognized using GRF and step length is calculated from the position of reflective markers attached on both heels at heel-strikes. The average body weight, leg length, and step length at different speeds are used as parameters for the model (Table 1). GRFs are normalized with respect to body weight and averaged to obtain the mean GRFs across all subjects for comparison.

The simulation results of each optimization trial are compared with the experimental measurements. Here we use GRF as the representative feature of walking patterns and calculate the correlation coefficient between model predictions and empirical data as the index of resemblance (Rebula and Kuo, 2015).

2.4. Model evaluation

In this actuated dissipative spring-mass model, the selection of three major parameters (k, c and α) will lead to different optimization results. To examine their influence on the gait solution, we first test each individual parameter separately and control the other two parameters using parameters listed in Table 1 at the speed of 1.25 m/s. Gait characteristics such as profiles and the maximal value of the vertical GRF (F_{gy-max}), stance time ($T_{stance} = T_{step} + T_{DS}$), and energy cost ($J_w$) are analyzed and compared with respect to the change of the parameter. We further manually tune these three parameters based on the observed impacts of each parameter and seek for parameter sets that achieve GRF visually close to the measured profiles at three different speeds.

3. Results

3.1. Effects of the stiffness

We tested 20 stiffness values ranging from 5×10^3 to 1×10^5N/m (Table 1). For simplicity, the damping value is set close to zero (to avoid zero power input) and the objective consists only of the energy cost ($\alpha = 0$). Vertical GRF from 5 representative stiffness values are shown in Fig. 2(A ~ E). It's observed that the GRF profiles changes from a one-peak shape, to a double-peak shape, then to a multiple-peak shape with an increase in k. The GRF profile is closest to the experimental results at a stiffness of 2×10^4 N/m, with a correlation coefficient of 0.969 (Fig. 3A). Additionally, with an increase of stiffness values, the energy cost (J_w) tends to slowly increase but is always at a low level (all less than 20 J, Fig. 3B). However, the stance time significantly decreases (from 0.687 to 0.513, Fig. 3C) while the maximal vertical GRF increases from 1.054 body weight (BW) to 2.680 BW (Fig. 3D).

3.2. Effects of the damping

20 damping values, ranging from 0 to 6×10^4 Ns/m^2 (Table 1), are examined with a stiffness value of 2×10^4 N/m and a weight of zero ($\alpha = 0$). With the increase of damping, the first peak in the vertical GRF tends to increase while the second peak will decrease, as shown in Fig. 2(F ~ J). The GRF also tends to get flatter,

Table 1
Parameters used in simulation trials. Body weight, leg length, (L_{leg}, from the trochanter to the ground) are measured before experiments. The equivalent pendulum length of the body can be taken as $1.20L_{leg}$ (Hof et al., 2005) and thus we use the maximal leg length of $(1.2L_{leg} + 0.1)$ in optimization. Step length is calculated from the position of heel markers at heel-strikes and the mean values at each speed are used in simulations. Three major model parameters are tested individually with the other two controlled at the speed of 1.25 m/s. A small damping value is used when testing stiffness and objective to ensure a non-zero energy cost.

Body weight (Kg)	69.7		
Maximal Leg length (m)	1.21		
Velocity (m/s)	1.00	1.25	1.50
Step length (m)	0.53	0.62	0.69
Conditions	Testing stiffness	Testing damping	Testing weight
Stiffness k (N/m)	5×10^3 to 1×10^5[a]	2×10^4	5×10^4
Damping c (Ns/m^2)	100	0 to 6×10^4 [b]	100
Weight α	0	0	0 to 1[c]

[a] 20 values were used: 5×10^3, 1×10^4, 1.5×10^4, 2×10^4, 2.5×10^4, 3×10^4, 3.5×10^4, 4×10^4, 4.5×10^4, 5×10^4, 5.5×10^4, 6×10^4, 6.5×10^4, 7×10^4, 7.5×10^4, 8×10^4, 8.5×10^4, 9×10^4, 9.5×10^4, 1×10^5.

[b] 20 values were used: 0, 1×10^3, 2.5×10^3, 5×10^3, 7.5×10^3, 1×10^4, 1.25×10^4, 1.5×10^4, 1.75×10^4, 2×10^4, 2.25×10^4, 2.5×10^4, 2.75×10^4, 3×10^4, 3.25×10^4, 3.5×10^4, 3.75×10^4, 4×10^4, 5×10^4, 6×10^4.

[c] 20 values were used: 0, 1×10^{-6}, 5×10^{-6}, 1×10^{-5}, 2.5×10^{-5}, 5×10^{-5}, 7.5×10^{-5}, 1×10^{-4}, 2.5×10^{-4}, 5×10^{-4}, 7.5×10^{-4}, 1×10^{-3}, 2.5×10^{-3}, 5×10^{-3}, 7.5×10^{-3}, 1×10^{-2}, 5×10^{-2}, 1×10^{-1}, 5×10^{-1}, 1.

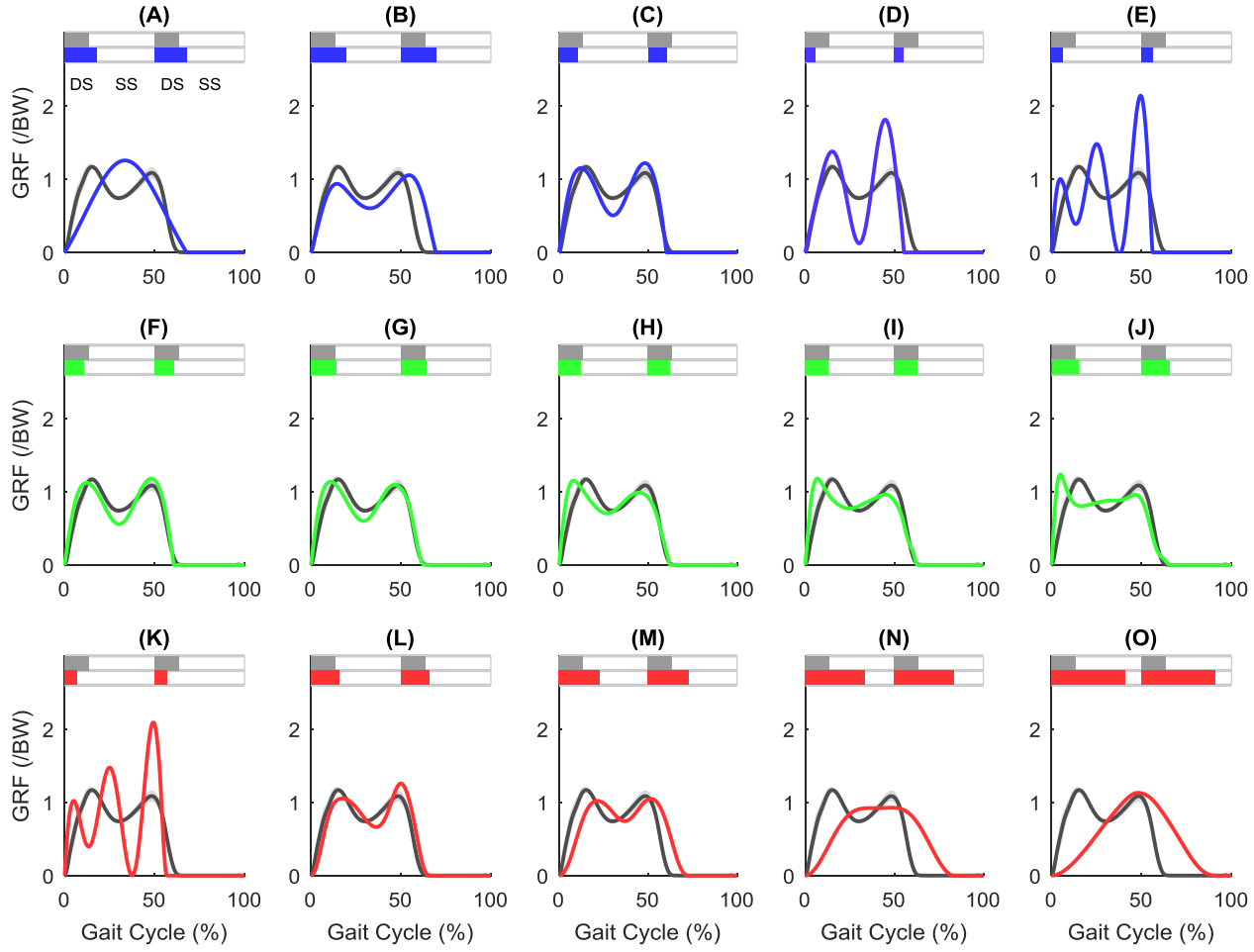

Fig. 2. The predicted vertical GRF at each trial with the experimental GRF shown for comparison. (A-E) are trials to test the stiffness where $k = 5 \times 10^3$, 1×10^4, 2×10^4, 3×10^4 and 5×10^4 N/m respectively. (F-J) are trials to test the damping where $c = 0$, 5×10^3, 1.5×10^3, 2.5×10^4 and 5×10^4 Ns/m^2 respectively. (K-O) are trials to test the weight where $\alpha = 0$, 7.5×10^{-4}, 1.5×10^{-3}, 2.25×10^{-3} and 1.0 respectively. The average experimental GRFs are shown in black lines with the shaded area showing ± 1 standard deviation. Lines in blue, green and red are GRFs predicted in each condition. (For interpretation of the references to color in this figure legend, the reader is referred to the web version of this article.)

especially around the mid-stance. However, the correlation coefficient slightly decreases with increased damping (Fig. 3A). Large damping values result in significantly higher energy cost (increase from 1.090 J to 61.352 J, Fig. 3B). A slight increase of stance time and maximal vertical GRF can also be found in Fig. 3 C-D.

3.3. Effects of the weight in objective

20 wt values, ranging from 0 to 1 (Table 1), are examined with a stiffness value of 5×10^4N/m and a damping value of 100 Ns/m^2. With an increase of weight value, the vertical GRF changes from three peaks to double peaks and then to a single peak (Fig. 2 (K $\sim$ O)), with the highest correlation coefficient of 0.963. Larger weight values result in higher energy cost and longer stance time (Fig. 3B and C). The change of weight introduces a rapid change of maximal vertical GRF when α is around 2.5×10^{-4} (Fig. 3 D).

3.4. Achieving more human-like walking patterns

As shown in Fig. 4, by tuning these three parameters, we can achieve very similar vertical GRF to experimental measurements, at all three walking speeds, with correlation coefficients of 0.983, 0.982 and 0.966 for 1.0, 1.25 and 1.5 m/s, respectively. For example, with the parameter set at 1.25 m/s ($k = 5 \times 10^4$, $c = 2 \times 10^4$ and $\alpha = 2.2 \times 10^{-4}$), the length of the spring-damping unit and actuator are shown in Fig. 5. The excursion of the actuator is much larger (0.041 m) than that of the spring (0.017 m). The profile of the spring and leg forces also show a double-peak shape similar to the vertical GRF. The profiles of leg power are also similar to those observed from experiments in literature (Donelan et al., 2002).

4. Discussion

In this paper, we introduce a spring-damping mechanism to the minimal biped model and propose an actuated dissipative spring-mass model that can achieve more human-like GRF patterns. This model contains three parameters representing three elements in the model: the stiffness, the damping, and the objective function. These three elements all help to achieve human-like GRF and have distinct effects.

Elasticity exists in human structures, such as muscle tendons, and various studies have verified the importance of elasticity in human walking and running (Alexander, 1992; Geyer and Herr, 2010). When setting c close to 0 and $\alpha = 0$, the energy cost is always close to zero: indicating the optimizer will largely take advantage of the energy-conservation as also observed in (Srinivasan, 2010). The increased number of peaks in GRF may be explained by the higher natural frequency along with the increase

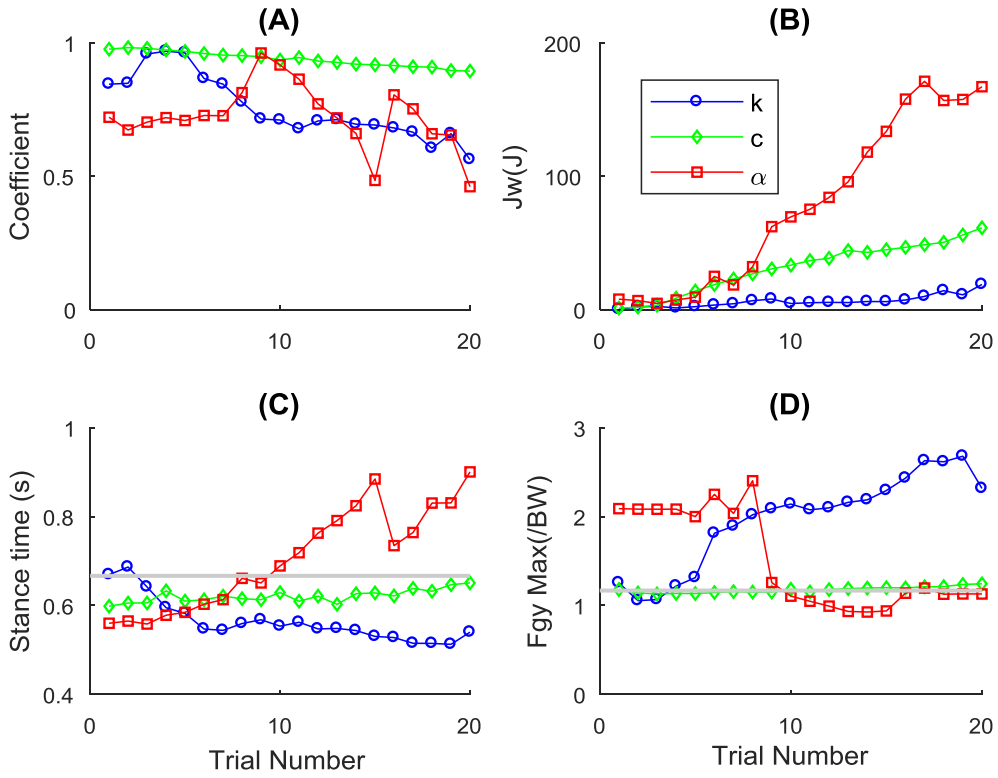

Fig. 3. Results of trials at different stiffness (k), damping (c) and weight values (α). (A) The correlation coefficient between the experimental vertical GRF and model predictions. (B) The energy cost (J_w), (C) the stance time and (D) the maximal vertical GRF at different conditions. The abscissa axis corresponds to the 20 trials in each condition.

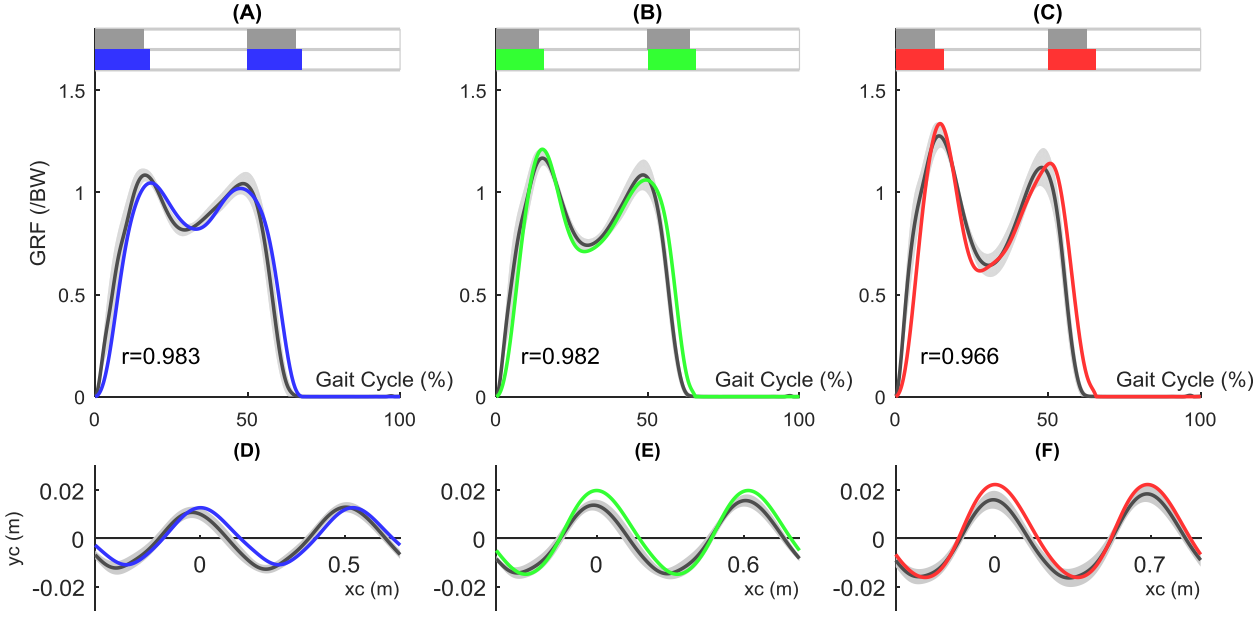

Fig. 4. Vertical GRFs that have the highest correlation coefficients with the experimental measurements in our examined trials for walking speeds (A) 1 m/s, $k = 4 \times 10^4$, $c = 1 \times 10^4$, $\alpha = 2.2 \times 10^{-4}$ (B) 1.25 m/s, , $k = 5 \times 10^4$, $c = 2 \times 10^4$, $\alpha = 2.2 \times 10^{-4}$ and (C) 1.5 m/s, , $k = 7 \times 10^4$, $c = 4.2 \times 10^4$, $\alpha = 1.9 \times 10^{-4}$. The corresponding trajectories of body center of mass are computed from GRF and are shown in (D-F). The experimental GRF and trajectories are shown in black with the area of ±1 standard deviation. Predictions are shown in blue, green and red color. (For interpretation of the references to color in this figure legend, the reader is referred to the web version of this article.)

of stiffness. Higher stiffness also results in larger peak GRF and shorter stance time (Fig. 3). With little energy input from the leg actuators, this model performs analogously to the SLIP model and shows large peaks and a deep trough in the vertical GRF (Fig. 2C and D). This feature can compensate for the drawback of the minimal biped model, which gives high force at mid-stance. As a result, the combination of the spring mechanism and minimal biped model can achieve "normal" magnitudes in GRF profiles.

Without using a spring mechanism, some previous models in literature converge to impulsive walking patterns when optimizing

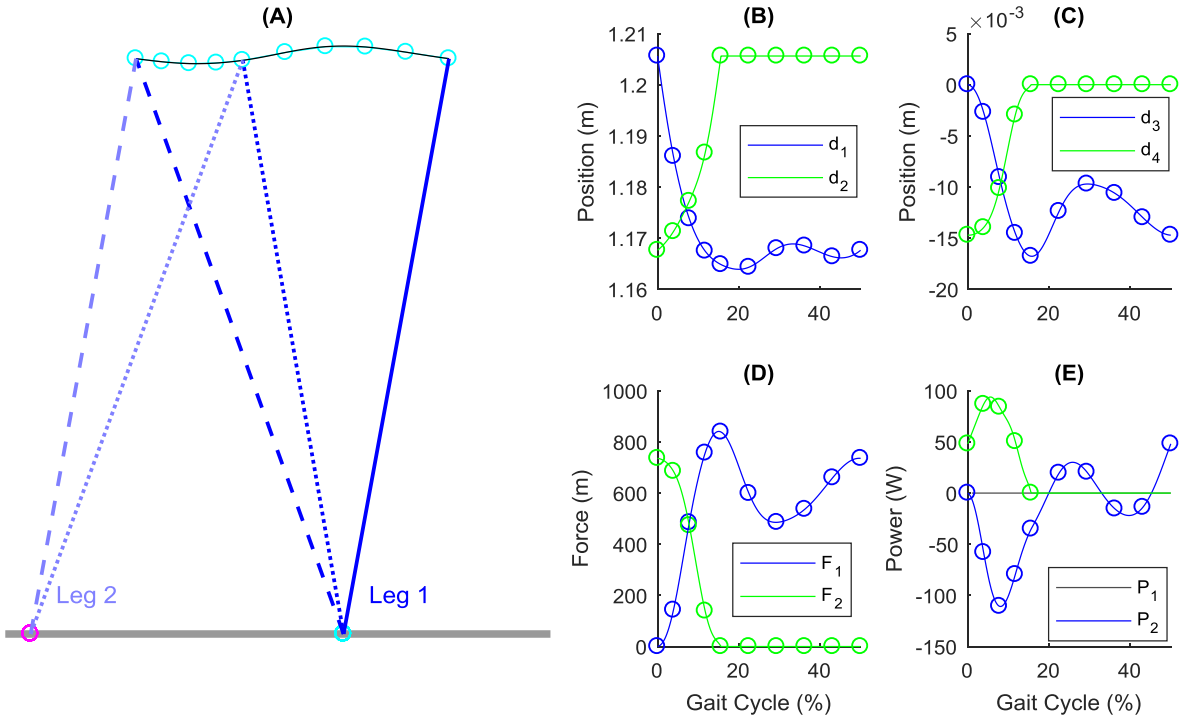

Fig. 5. Predicted walking pattern with a high correlation coefficient at 1.25 m/s. (A) the body trajectory, (B) actuator length, (C) spring length, (D) leg forces and (E) leg power are shown in a step cycle.

mechanical work (Hasaneini et al., 2013). Some other models choose different optimizing objectives such as torque to avoid the impulsive walking pattern (Martin and Schmiedeler, 2014). More complex models that contain muscles as actuators already include the springy structure. For example, the commonly used Hill-type muscles contain elastic elements in their model (Ackermann and van den Bogert, 2010; Miller, 2014; Song and Geyer, 2015). Indeed, optimizing energy cost in their models no longer shows an impulsive pattern. With a proper objective function or control, a complex model without the spring mechanism may replicate human walking patterns. However, the spring is still a simple and effective element in achieving human-like walking.

Adding a damping unit to a spring means there will be energy loss along with the length change of the spring, making the model dissipative. The damping unit shouldn't be used in periodical walking, when there is no actuation to compensate for energy loss of damping, as in the SLIP model. A significant influence of damping is changing the relative size of the two peaks in the vertical GRF. When the damping is zero, the first peak is of similar magnitude or smaller than the second peak (Fig. 2F). With an increase of damping, the second peak reduces and the trough gets shallower. Interestingly, the damping value has little impact on the stance time and maximal vertical GRF (Fig. 3). It's unclear whether the actual GRF peak difference in human walking is truly related to the damping since other human structures such as shaped feet and different muscles may also account for the difference. Although there is no damping element In classic Hill-type muscles (Robertson et al., 2013), the force-velocity property of the muscle itself may behave as a damping property (lower force at higher shortening velocity).

The objective function plays an essential and influential role in this optimization-based biped model. Since human walking is found to be largely governed by energetics, humans tend to walk in a manner minimizing energy cost (Ralston, 1958; Donelan et al., 2001). However, in springless models, optimizing the mechanical work usually gives an impulsive walking pattern (Srinivasan and Ruina, 2006; Hasaneini et al., 2013), which is unrealistic as human can only generate finite forces. When stiffness and damping elements are included, as in our model, purely minimizing the energy cost ($\alpha = 0$) does not give predictions close to experimental results. In this case, the vertical GRF still displayed large peaks. Adding a cost from the leg forces' second derivative, as used in (Rebula and Kuo, 2015), can help to reduce the excessively large peak forces and the number of peaks (Fig. 2), resulting in very similar GRF profiles as observed in experiments. Larger weight value will reduce the number of peaks and increase the stance time (Fig. 3C), opposite to the effect of stiffness value. Even though the real objective of a human is unclear, we infer that a human may not desire a large force variation rate.

By tuning these three model parameters, this simple model can achieve human-like GRF patterns, verifying our hypothesis that combining the SLIP model and the minimal biped model can reach a more human-like walking model. This model can help us to further understand fundamental biomechanics of human walking. The simplicity is advantageous for examining the function of individual parameters and makes it easier to even manually tune the model, which could be much harder, or even impossible in highly complex muscular-skeletal models. This new model may also change some understandings of human walking from previous models. For example, the stiffness values that achieve human-like GRF pattern are much higher than those identified based on spring-damper models (Zhang et al., 2000) or SLIP models (Kim and Park, 2011). We believed the values found in this paper may be more rational and close to the real values of elastic components in the body since actuators were not included in those models. Besides, the experimentally measured stiffness of elastic components in human legs is also quite high. For example, the stiffness of Achilles tendon is around 1.3×10^5 N/m according to measurements in (Kubo et al., 2007). The computed optimal gastrocnemius tendon stiffness is also around $1.5–5 \times 10^5$ N/m (Lichtwark and Wilson, 2008). Indeed, it should be noted that the stiffness in the model is a combination of all elastic components in the leg rather

than a specific structure, which may be hard to measure or compare.

Although the model-predicted GRF matched well with the empirical results, some limitations still exist. This model is a much-simplified abstraction of a human and thus some characteristics of human walking cannot be achieved by this model. For example, telescope actuators are set along the legs and the non-axial force, which may produce considerable work (Maykranz et al., 2013), are neglected. With the massless legs and zero leg-swing cost, the step length cannot be optimized. Energy-related gait features such as the preferred walking speed and preferred step frequency may not be realized (Saibene and Minetti, 2003) as discussed in Supplementary Materials. The exact biological sources of the stiffness and damping in our model are still unclear. Therefore, further interpretation of this model should be made cautiously. Other objective functions may achieve even better performance and could be further explored. The constraint of maximal leg length may also affect the optimization solution quantitatively. In the comparison process, we used the average GRF profiles of multiple steps and multiple subjects at each speed as the reference for comparison. However, during human walking, variations between steps and individual differences are omitted and may need to be considered in future work.

Acknowledgment

This work was supported in part by the NSFC Grant No. 51775485 and U1613203, the Zhejiang Provincial Natural Science Foundation of China under Grant No. LR15E050002, the State Key Laboratory of Fluid Power and Mechatronic Systems under Grant GZKF-201702 to T. Liu, an NSERC Discovery Grant to Q. Li, and a fellowship from the Chinese Scholarship Council to T. Li. We also thank Jean-Paul Martin for his help in editing this paper.

Conflict of interest statement

The authors state no conflicts of interest.

Appendix A. Supplementary material

Supplementary data to this article can be found online at https://doi.org/10.1016/j.jbiomech.2019.04.028.

References

Ackermann, M., van den Bogert, A.J., 2010. Optimality principles for model-based prediction of human gait. J. Biomech. 43 (6), 1055–1060.
Alexander, R.M., 1992. A model of bipedal locomotion on compliant legs. Philos. Trans. Roy. Soc. B: Biol. Sci. 338 (1284), 189–198.
Alexander, R.M., 1995. Simple models of human movement. Appl. Mech. Rev. 48 (8), 461–470.
Anderson, F.C., Pandy, M.G., 2001. Dynamic optimization of human walking. J. Biomech. Eng. 123 (5), 381–390.
Bellman, R.E., 2003. Dynamic Programming. Courier Dover Publications.
Cavagna, G.A., Thys, H., Zamboni, A., 1976. The sources of external work in level walking and running. J. Physiol. 262 (3), 639–657.
Donelan, J.M., Kram, R., Kuo, A.D., 2001. Mechanical and metabolic determinants of the preferred step width in human walking. Proc. Roy. Soc. B: Biol. Sci. 268 (1480), 1985–1992.
Donelan, J.M., Kram, R., Kuo, A.D., 2002. Simultaneous positive and negative external mechanical work in human walking. J. Biomech. 35 (1), 117–124.
Flores, P., Lankarani, H.M., 2016. Contact Force Models for Multibody Dynamics. Springer International Publishing Switzerland.
Garcia, M., Chatterjee, A., Ruina, A., Coleman, M., 1998. The simplest walking model: stability, complexity, and scaling. J. Biomech. Eng. 120 (2), 281–288.
Geyer, H., Herr, H., 2010. A muscle-reflex model that encodes principles of legged mechanics produces human walking dynamics and muscle activities. IEEE Trans. Neural Syst. Rehabil. Eng. 18 (3), 263–273.
Geyer, H., Seyfarth, A., Blickhan, R., 2006. Compliant leg behaviour explains basic dynamics of walking and running. Proc. Roy. Soc. B: Biol. Sci. 273 (1603), 2861–2867.
Hasaneini, S.J., Macnab, C.J.B., Bertram, J.E.A., Leung, H., 2013. The dynamic optimization approach to locomotion dynamics: Human-like gaits from a minimally-constrained biped model. Adv. Rob. 27 (11), 845–859.
Hicks, J.L., Uchida, T., Seth, A., Rajagopal, A., Delp, S.L., 2015. Is my model good enough? Best practices for verification and validation of musculoskeletal models and simulations of movement. J. Biomech. Eng.-Trans. ASME 137 (2). 020905-020905.
Hof, A.L., Gazendam, M.G., Sinke, W.E., 2005. The condition for dynamic stability. J. Biomech. 38 (1), 1–8.
Hunt, K.H., Crossley, F.R.E., 1975. Coefficient of restitution interpreted as damping in vibroimpact. J. Appl. Mech.-Trans. ASME 42 (2), 440–445.
Kim, S., Park, S., 2011. Leg stiffness increases with speed to modulate gait frequency and propulsion energy. J. Biomech. 44 (7), 1253–1258.
Kubo, K., Morimoto, M., Komuro, T., Tsunoda, N., Kanehisa, H., Fukunaga, T., 2007. Influences of tendon stiffness, joint stiffness, and electromyographic activity on jump performances using single joint. Eur. J. Appl. Physiol. 99 (3), 235–243.
Kuo, A.D., 2001. A simple model of bipedal walking predicts the preferred speed–step length relationship. J. Biomech. Eng.-Trans. ASME 123 (3), 264–269.
Kuo, A.D., 2002. Energetics of actively powered locomotion using the simplest walking model. J. Biomech. Eng.-Trans. ASME 124 (1), 113–120.
Lichtwark, G.A., Wilson, A.M., 2008. Optimal muscle fascicle length and tendon stiffness for maximising gastrocnemius efficiency during human walking and running. J. Theor. Biol. 252 (4), 662–673.
Margaria, R., 1976. Biomechanics and Energetics of Muscular Exercise. Clarendon Press, Oxford, England.
Martin, A.E., Schmiedeler, J.P., 2014. Predicting human walking gaits with a simple planar model. J. Biomech. 47 (6), 1416–1421.
Maykranz, D., Grimmer, S., Seyfarth, A., 2013. A work-loop method for characterizing leg function during sagittal plane movements. J. Appl. Biomech. 29 (5), 616–621.
Mcgeer, T., 1990. Passive dynamic walking. Int. J. Rob. Res. 9 (2), 62–82.
McGrath, M., Howard, D., Baker, R., 2015. The strengths and weaknesses of inverted pendulum models of human walking. Gait Posture 41 (2), 389–394.
Miller, R.H., 2014. A comparison of muscle energy models for simulating human walking in three dimensions. J. Biomech. 47 (6), 1373–1381.
Pappalardo, A., Albakri, A., Liu, C., Bascetta, L., De Momi, E., Poignet, P., 2016. Hunt–crossley model based force control for minimally invasive robotic surgery. Biomed. Signal Process. Control 29, 31–43.
Ralston, H.J., 1958. Energy-speed relation and optimal speed during level walking. Internationale Zeitschrift fur angewandte Physiologie, einschliesslich Arbeitsphysiologie 17 (4), 277–283.
Rebula, J.R., Kuo, A.D., 2015. The cost of leg forces in bipedal locomotion: a simple optimization study. Plos One 10 (2), e0117384.
Ren, L., Jones, R.K., Howard, D., 2005. Dynamic analysis of load carriage biomechanics during level walking. J. Biomech. 38 (4), 853–863.
Robertson, D.G.E., Caldwell, G.E., Hamill, J., Kamen, G., Whittlesey, S.N., 2013. Research methods in biomechanics. second ed.
Rummel, J., Blum, Y., Maus, H.M., Rode, C., Seyfarth, A., 2010. Stable and robust walking with compliant legs. In: IEEE International Conference on Robotics and Automation (ICRA), pp. 5250–5255.
Saibene, F., Minetti, A.E., 2003. Biomechanical and physiological aspects of legged locomotion in humans. Eur. J. Appl. Physiol. 88 (4–5), 297–316.
Song, S., Geyer, H., 2015. A neural circuitry that emphasizes spinal feedback generates diverse behaviours of human locomotion. J. Physiol.-London 593 (16), 3493–3511.
Srinivasan, M., 2010. Fifteen observations on the structure of energy-minimizing gaits in many simple biped models. J. R. Soc. Interface 8 (54), 74–98.
Srinivasan, M., Ruina, A., 2006. Computer optimization of a minimal biped model discovers walking and running. Nature 439 (7072), 72–75.
Whittle, M., 2007. Gait Analysis, An Introduction. Butterworth-Heinemann Elsevier.
Winter, D.A., 2009. Biomechanics and Motor Control of Human Movement. John Wiley & Sons Inc.
Xiang, Y.J., Arora, J.S., Chung, H.J., Kwon, H.J., Rahmatalla, S., Bhatt, R., Abdel-Malek, K., 2012. Predictive simulation of human walking transitions using an optimization formulation. Struct. Multidiscip. Optim. 45 (5), 759–772.
Zhang, L., Xu, D., Makhsous, M., Lin, F., 2000. Stiffness and viscous damping of the human leg. In: Proceedings of the 24th Annual Meeting of the American Society of Biomechanics, Chicago, IL.